The Astrophysical Journal, 825:118 (6pp), 2016 July 10 doi:10.3847/0004-637X/825/2/118

THE REALM OF THE GALACTIC GLOBULAR CLUSTERS AND THE MASS OF THEIR PRIMORDIAL CLOUDS

Guillermo Tenorio-Tagle[1], Casiana Muñoz-Tuñón[2], Santi Cassisi[3], and Sergiy Silich[1]
[1] Instituto Nacional de Astrofísica Óptica y Electrónica, AP 51, 72000 Puebla, México; gtt@inaoep.mx
[2] Instituto de Astrofísica de Canarias, E38200, Tenerife, Spain; cmt@iac.es
[3] INAF—Astronomical Observatory of Collurania, via M. Maggini, I-64100 Teramo, Italy; cassisi@oa-teramo.inaf.it
Received 2016 February 19; revised 2016 May 5; accepted 2016 May 8; published 2016 July 11

ABSTRACT

By adopting the empirical constraints related to the estimates of helium enhancement (ΔY), the present mass ratio between first and second stellar generations (M_{1G}/M_{2G}), and the actual mass of Galactic globular clusters (M_{GC}), we envisage a possible scenario for the formation of these stellar systems. Our approach allows for the possible loss of stars through evaporation or tidal interactions and different star-formation efficiencies. In our approach, the star-formation efficiency of the first generation (ϵ_{1G}) is the central factor that links the stellar generations because it not only defines both the mass in stars of the first generation and the remaining mass available for further star formation, but it also fixes the amount of matter required to contaminate the second stellar generation. In this way, ϵ_{1G} is fully defined by the He enhancement between successive generations in a GC. We also show that globular clusters fit well within a ΔY versus M_{1G}/M_{2G} diagram that indicates three different evolutionary paths. The central one is for clusters that have not lost stars through tidal interactions from either of their stellar generations, and thus their present M_{GC} value is identical to the amount of low-mass stars ($M_* \leqslant 1\,M_\odot$) that resulted from both stellar generations. Other possible evolutions imply either the loss of first-generation stars or the combination of a low star-formation efficiency in the second stellar generation and a loss of stars from the second generation. From these considerations, we derive a lower limit to the mass (M_{tot}) of the individual primordial clouds that gave origin to globular clusters.

Key words: globular clusters: general – hydrodynamics

1. INTRODUCTION

During the last decade, one of the most astonishing results in the context of stellar astrophysics has been the discovery of the multiple population phenomenon in Galactic globular clusters (GGCs), that is, the presence of distinct subpopulations characterized by their specific chemical patterns (Bedin et al. 2004; Marino et al. 2008, 2012; Carretta et al. 2009; Bellini et al. 2010; Piotto et al. 2012; Renzini et al. 2015, and references therein).

The most distinctive chemical features that characterize the various stellar populations in a given GC are the presence of different abundances of light elements (such as C, N, O, and Na) and different levels of He enhancement, from extremely small $\Delta Y \approx 0.01$ (Milone et al. 2012c; Piotto et al. 2013) to huge values ≈0.15 (Norris 2004; Piotto et al. 2005, 2007; King et al. 2012; Bellini et al. 2013). These distinct chemical patterns among the various subpopulations in the same cluster create the well-known O–Na anticorrelation that is—from a chemical point of view—the most evident property of the multiple population phenomenon (see, e.g., Gratton et al. 2012; Marino et al. 2014).

At the same time, very accurate photometric investigations performed using the *Hubble Space Telescope* have revealed the existence of multiple evolutionary sequences in the color–magnitude diagrams (CMDs) of various GCs, such as distinct main sequence (MS), subgiant branch, and multiple red giant branch loci. Actually, the features observed in the CMD change significantly from cluster to cluster, and their properties strongly depend on the adopted photometric systems (see Milone et al. 2010, 2012b, 2013, 2015, and references therein).

The most common—although still debated—scenarios postulate that, in any GC, a second (and in some cases also more) generation of stars can form from the ejecta of intermediate-mass or massive stars belonging to the first stellar population, whose initial chemical composition is modified by high-temperature proton captures. However, some amount of dilution between pristine (unpolluted) matter and matter processed through thermonuclear burning seems to be unavoidable in order to explain the trend of the chemical patterns observed, for instance, along the O–Na anticorrelation diagram (see the discussion in D'Ercole et al. 2011 and Renzini et al. 2015).

The ability to trace both spectroscopically and photometrically the various subpopulations hosted by each individual GC allows now for the identification of both the primordial stellar component (the first generation, 1G) and the second-generation (2G) stars. At the same time, the strong correlation that exists between the spectroscopic signatures of the distinct subpopulations and their distribution along the multiple CMD sequences clearly indicates that the peculiar chemical patterns of 2G stars have to affect both the evolutionary properties of these stars and their spectral energy distributions (Sbordone et al. 2011; Cassisi et al. 2013a, 2013b; Dotter et al. 2015).

Although the photometric and spectroscopic properties of the subpopulations in the GGC sample are nowadays well known, we still face a *plethora* of issues related to many aspects of the multiple population phenomenon, the most important ones being (1) the nature of the polluters, that is, the type of stars responsible for the nucleosynthesis at the base of the 2G chemical patterns, and (2) how 2G stars were actually able to form in the inner regions of GGCs, that is, in a region with a very high stellar density; (3) the current fraction of 2G to 1G stars observed in an individual cluster raises the mass budget problem; that is, since the candidate polluting stars make up

only a very small fraction of the total initial mass of the GC, currently observed 1G stars (and their already evolved companions) are not enough to have produced the required amount (also accounting for dilution) of enriched matter for a 2G. For a detailed review of the various problems related to the interpretation of the multiple population phenomenon in GGCs, we refer to the work by Renzini et al. (2015), Bastian et al. (2015), and Bastian & Lardo (2015) and references therein. Because of the existence of all these issues related to the explanation of this phenomenon, it is mandatory to fully exploit the empirical constraints derived from the ongoing spectroscopic and photometric surveys (e.g., Piotto et al. 2015) in order to obtain the most reliable possible set of constraints on the mass of the cluster progenitor, the star-formation efficiency for the various subpopulations, and an estimate of the capability of the various clusters to retain stars belonging to the distinct subpopulations.

Here we use current empirical estimates of the actual cluster mass and the relative fraction of 1G and 2G stars, as well as current estimates of the He enhancement between the various subpopulations in a sample of GGCs, in order to provide some clues on the total mass of the primordial cloud and at the same time on the possible evolutionary paths—in terms of the star-formation efficiency and the capability of clusters to retain the stars of the various subgroups—followed by the clusters in our sample.

2. SECONDARY STELLAR GENERATIONS IN GGCs

Let us assume a massive cloud with a total mass $M_{\rm tot}$ that collapses and forms a first stellar generation with an efficiency $\epsilon_{\rm 1G}$. We also assume that the event leads to a full Kroupa (2001) initial mass function (IMF) with stars in the range 0.1–120 $M_\odot$, and, as expected from massive starbursts restricted to a small volume, a large fraction of their massive stars should end up as interacting binaries (see de Mink et al. 2009; Schneider et al. 2014). The major implication of this (as in de Mink et al. 2009; Izzard et al. 2013) is that, instead of massive stars producing powerful winds during their entire life, most of their H-burning products would exit the stars with a low velocity (approximately a few tens of km s^{-1}), and thus, during the early evolution, the large collection of massive binaries is likely to hold the remaining cloud against gravitational collapse while contaminating the gas left over from star formation without disrupting its centrally concentrated density distribution. This latter point is also an important issue because, under such conditions, the blast waves from sequential supernovae (SNe) are all likely to undergo blowout, the sudden acceleration of the blast wave and of its shell of swept-up matter as soon as they enter the steep density gradient present in the remaining cloud. Such events lead to Rayleigh–Taylor instabilities in the swept-up shells and to their fragmentation, favoring the venting of the SN debris out of the remaining cloud without causing its contamination[4] (Krause et al. 2012; Tenorio-Tagle et al. 2015). Only the most massive clouds with a mass $M_{\rm gas} \geqslant 10^6\,M_\odot$ would be able to retain the high-velocity ejecta of a few percent of the SN explosions from the first generation, and only if these explode near the center of the gas distribution. In these latter cases, the mass available for a second stellar generation would also be contaminated with SN products, and its resultant stars will be likely to show a prominent Fe spread instead of the uniform metallicity characteristic of less-massive clusters (see the discussion in Marino et al. 2011; Milone et al. 2015, and references therein).

All these conditions here assumed seem to be at work in young, massive compact clusters such as NGC 5253, II Zw 40, and Henize 2–10, all completely buried in their natal clouds, which only allow for their detection at infrared and millimeter wavelengths (see Beck 2015; Turner et al. 2015, and references therein). These assumptions seem a reasonable possibility to justify secondary stellar generations in the young compact clusters such as NGC 1569-A, NGC 1569-B, and NGC 1705-1 (see Larsen et al. 2011), for which their resolved *Hubble Space Telescope* (*HST*) Advanced Camera for Survey photometry implies secondary stellar generations separated from their first generations by an age of less than 50 Myr.

Following gravitational collapse, the mass in stars of the first stellar generation is

$$M_{\rm 1G} = \epsilon_{\rm 1G} M_{\rm tot}. \quad (1)$$

If one accounts for tidal interactions and the possible loss of stars during the lifetime of a GC, then one can multiply Equation (1) by $\alpha_{\rm 1G}$ ($\leqslant$1) to account for the fraction of first-generation stars that are never lost from the cluster and contribute to the present mass.

We shall further assume that the leftover gas becomes thoroughly contaminated by the H-burning products shed by stars from the first stellar generation. The resultant He enhancement Y in the leftover cloud is then

$$Y = \frac{M_p Y_p + M_c Y_c}{(M_p + M_c)}, \quad (2)$$

where the subscripts p and c stand for the pristine and the contaminated gas, respectively. Following de Mink et al. (2009), the total mass of the contaminated gas amounts to $\sim$0.15 $M_{\rm 1G}$, which accounts for the fraction of the stellar mass shed by interacting massive binaries from the 1G. Thus the contaminated mass is $M_c = 0.15 M_{\rm 1G} = 0.15\epsilon_{\rm 1G} M_{\rm tot}$, and the mass in pristine gas after the 1G has formed is $M_p = (1 - \epsilon_{\rm 1G}) M_{\rm tot}$.

In this way, the resultant value of Y is

$$Y = \frac{(1 - \epsilon_{\rm 1G}) Y_p + 0.15\epsilon_{\rm 1G} Y_c}{(1 - \epsilon_{\rm 1G}) + 0.15\epsilon_{\rm 1G}}, \quad (3)$$

and the corresponding value of ΔY is

$$\Delta Y = Y - Y_p = \frac{0.15\epsilon_{\rm 1G}(Y_c - Y_p)}{(1 - \epsilon_{\rm 1G} + 0.15\epsilon_{\rm 1G})}. \quad (4)$$

This is plotted in Figure 1 as a function of $\epsilon_{\rm 1G}$, assuming, as in de Mink et al. (2009) and in Bastian et al. (2013), that $Y_c = 0.64$[5] and the primordial He abundance Y_p is equal to 0.24. Within this framework, a strong dilution of the contaminated mass happens naturally for cases with small values of $\epsilon_{\rm 1G}$, leading to small values of ΔY, and, conversely,

[4] It is worth noting that a different scenario has been recently envisaged by Calura et al. (2015) on the basis of 3D hydrodynamic simulations. In this scenario, the integrated feedback from stellar winds and SNe explosions would be responsible for the pristine gas removal within $\sim$14 Myr since the cluster formation.

[5] This value corresponds to the extreme He abundance in the ejecta of their model. However, as we discuss in the following, a change in this value could be easily accounted for in the analysis performed in this work.

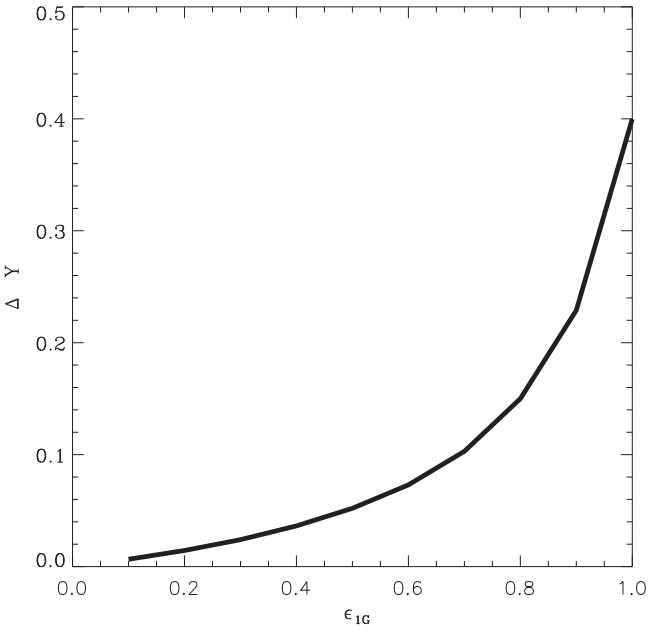

Figure 1. ΔY vs. the star-formation efficiency of the first stellar generation (ϵ_{1G}).

very little dilution is achieved in cases with a large ϵ_{1G}, causing large values of ΔY. We note that this expected trend leads to a range of ΔY values in good agreement with the range inferred from observations of GGCs, as we discuss in the following.

Within the framework here described, the efficiency of star formation of the first stellar generation (ϵ_{1G}) is what defines both the total amount of pristine gas left over from the formation of a first stellar generation and the mass of the contaminated gas ($0.15M_{1G}$), leading, upon a thorough mixing, to a contaminated cloud ready to trigger a second stellar generation with its own He abundance $Y_{2G} = Y_p + \Delta Y$ (see Equations (3) and (4) and Figure 1). From Equations (2)–(4) and the values of Y_p and Y_c there given, ϵ_{1G} is

$$\epsilon_{1G} = \frac{\Delta Y}{0.06 + 0.85\Delta Y}, \tag{5}$$

and thus it is fully defined by the observations. For those clusters hosting distinct subpopulations, each with a specific value of Y, Equation (5) should be replaced by $\epsilon_{(j-1)G} = \Delta Y_{j,j-1}/(0.15(0.64 - Y_{j-1}) + 0.85\Delta Y_{j,j-1})$ if the contaminant Y_c is 0.64 (as we used for massive binaries) and ΔY is measured between generation j and j–1. In this way, the ΔY values between subsequent generations would lead to the efficiency of star formation of all but the last stellar generation.

In the present analysis, we rely on the prescription for Y_c and the fraction of the total 1G mass available as contaminant gas, as provided by de Mink et al. (2009) in their scenario of interacting, massive binary systems. However, we note that this scenario is based on only one model, so additional computations are strongly needed, and *also* that this scenario, as well as other candidate polluters suggested so far, has its own shortcomings, as discussed by Bastian et al. (2015) and Renzini et al. (2015). Notwithstanding, in the present analysis we perform an exploratory analysis using these model predictions at face value. In principle, one could select a different polluter, but only if it does not disrupt the cloud left over from star formation. The implementation requires us only to replace in our equations the corresponding values of M_c and Y_c. The same consideration could be applied to the case of AGB stars (D'Antona et al. 2002), but not if the model assumes the loss of the matter left over from the formation of a first stellar generation $(1–\epsilon_{1G})M_{tot}$ as in D'Ercole et al. (2008), as such an assumption invalidates our Equations (3)–(5). Note that, in the scenario of AGB stars as candidate polluters, the amount of pristine gas that has to be accreted in order to dilute the AGB stellar ejecta is a free parameter, whereas in the present analysis, the diluter gas is simply the residual gas from 1G formation.

In our approach, the total mass available for a second stellar generation (2G) is

$$M_{\text{residual gas}} = (1 - \epsilon_{1G})M_{tot} + 0.15M_{1G}, \tag{6}$$

where the second term accounts for the mass that contaminates the gas left over from the formation of the 1G. Having all this mass already in place, there is no need to invoke, as in other scenarios for GC formation, the accretion of further pristine gas to dilute the cloud that would give origin to a second stellar generation.

As in Equation (1), this equation has to be multiplied by a star-formation efficiency factor (ϵ_{2G}) to infer the mass of the second stellar generation. Also, if one is to consider the possible loss of stars through tidal interactions, Equation (6) should also be multiplied by the fraction of stars from the second generation that remain gravitationally trapped within the cluster ($\alpha_{2G} \leqslant 1$) and contribute to its present mass M_{2G}. However, α_{2G} should have a value close to 1, given the empirical evidence showing the 2G being commonly centrally concentrated with respect to the 1G (see the analysis performed by Bellini et al. 2009; Lardo et al. 2011; Milone et al. 2012b, 2012a, 2013, 2015).[6]

After some algebra, Equations (1), (4), and (6) yield

$$X = \frac{M_{1G}}{M_{2G}} = \frac{\epsilon_{1G}\alpha_{1G}}{\epsilon_{2G}\alpha_{2G}(1 - \epsilon_{1G} + 0.15\epsilon_{1G})} = \frac{\Delta Y\gamma}{0.15(Y_c - Y_p)} \tag{7}$$

where

$$\gamma = \frac{\alpha_{1G}}{\alpha_{2G}\epsilon_{2G}} = \frac{0.15(Y_c - Y_p)X}{\Delta Y} = \frac{0.06X}{\Delta Y}, \tag{8}$$

and thus γ is also constrained by the observations. From the above equation, $\Delta Y = 0.06X/\gamma$. This is plotted on Figure 2 against the mass ratio M_{1G}/M_{2G}, where the solid line depicts the case when $\gamma = 1$. All clusters located to the right of the solid line have a γ larger than one, whereas those to the left have a γ smaller than one. For example, the dotted lines in Figure 2 correspond to values of $\gamma = 1.4$ and 3.3, whereas the dashed lines correspond to $\gamma = 0.5$ and 0.7.

The three variables (α_{1G}, α_{2G}, and ϵ_{2G}) cause a degeneracy in Equations (7) and (8). Nevertheless, the position of a stellar cluster in the $\Delta Y - M_{1G}/M_{2G}$ parameter space allows one to draw some conclusions regarding its formation and evolution. For example, all clusters to the right of the solid line have the product $\alpha_{2G}\,\epsilon_{2G}$ smaller than α_{1G}. This implies that in all such clusters the second generation was formed with a small

[6] But see also Dalessandro et al. (2014) for the case of a lack of radial gradients in the stellar populations of NGC 6362.

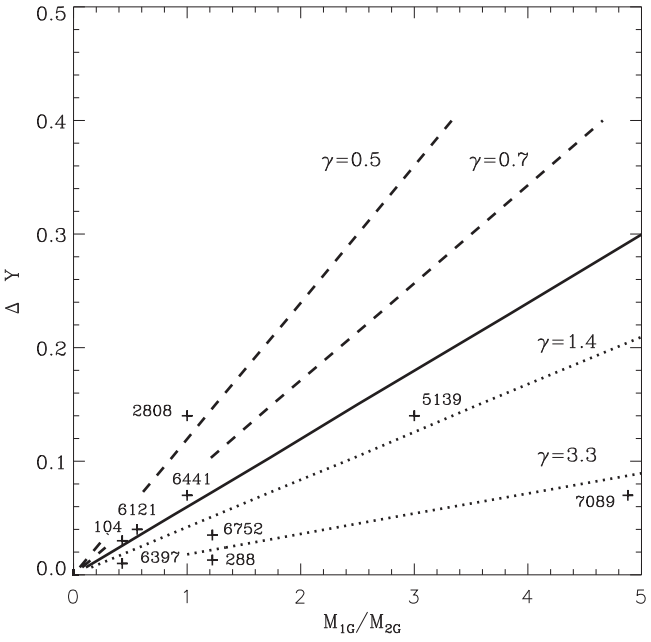

Figure 2. The realm of the GGCs: ΔY vs. M_{1G}/M_{2G} for a sample of Galactic globular clusters. The solid line presents the results from Equations (4) and (7) assuming α_{1G}, α_{2G}, and ϵ_{2G} all being equal to 1. The dashed lines to the left of the solid line are also from Equation (7) but for different values of γ (0.7 and 0.5). The dotted lines to the right of the solid line are from Equation (7) but with the product $\alpha_{2G}\,\epsilon_{2G}$ equal to 0.7 and 0.3, which leads to γ values equal to 1.4 and 3.3. The symbols represent the data for a sample of GGCs with their NGC identification number.

efficiency, $\epsilon_{2G} < \alpha_{1G} < 1$, as the value of α_{2G} should be close to 1. On the other hand, all clusters to the left of the solid line in Figure 2 have $\alpha_{1G} < \epsilon_{2G} < 1$ (as $\alpha_{2G} \approx 1$), which implies that during the evolution such clusters lost a significant fraction of their first-generation stars.

In Figure 2 we also show empirical data for a sample of Galactic GCs (Milone et al. 2012b, 2014, 2015, and references therein). From these studies one knows three different variables for each cluster: the value of ΔY, the total present mass of the clusters (M_{GC}), and the ratio of the number of stars from a 2G to the total number: $N_2/N_{tot} = A$. From the latter we know that $N_2 = AN_{tot}$, and if $N_{tot} = N_1 + N_2$, then $N_1/N_2 = (1 - A)/A$. Given the extended evolution of GCs, we know one is dealing today with stars within the same mass range ($\leqslant 1\,M_\odot$), and thus such a ratio is equivalent to the mass ratio $X = M_{1G}/M_{2G}$, as plotted in Figure 2. Before discussing what kind of information we can extract by comparing the empirical data set with our model, we wish to comment about the reliability of the adopted, empirical estimates for the 2G to 1G population ratio. When comparing the estimates, currently available in the literature, of N_2/N_1 for a given cluster, one can easily find significant differences. For instance, Carretta et al. (2009), on the basis of the Na–O anticorrelation in 15 GCs, conclude that the mass of 1G in GCs amounts to about 30% of the total mass, what they call the intermediate population amounts to almost 60%, and in some clusters there is an extra ~10% in extreme population (a similar conclusion has been obtained by Bastian & Lardo 2015). Seven of their GCs coincide with our sample. However, in the data in our Figure 2 (and in Table 1), five of the GCs in our sample have a 1G mass larger than the mass of the 2G. Two have an equal mass, and only three of them have a 2G more massive than the 1G. It is also true that two (NGC 7089 and NGC 5139) of our clusters with a 1G more populous than the 2G are not included in the original sample by Carretta et al. (2009).

The estimates we are using in this work are taken from photometric surveys that consider a much larger number of stars with respect the spectroscopic surveys. In addition, usually the spectroscopy surveys are limited to GC outskirts, whereas *HST*-based photometric surveys also sample the inner core of the GCs, so the presence of a radial gradient could also help in explaining the difference in the estimates of the N_2/N_1 ratio.[7]

In Table 1 we list the observed and derived parameters for nine GGCs. Column 1 gives their NGC identification number, and columns 2–4 give the He enhancement ΔY, the derived M_{1G}/M_{2G} as obtained from the observed values N_2/N_{tot}, and their present mass in solar masses (M_{GC}). Column 5 gives the values of ϵ_{1G} as derived from Equation (5), while columns 6–9 report the present masses M_{1G} and M_{2G}, the predicted values of γ (from Equation (8)), and the lower-limit value for M_{tot}, respectively.

3. THE MASS OF THE PRIMORDIAL CLOUDS

From the present values of M_{1G}/M_{2G} and the estimated mass of a GC, one can infer the present mass of both the first and second generation:

$$M_{2G} = \frac{M_{GC}}{X+1} \qquad \text{and} \qquad M_{1G} = M_{GC} - M_{2G}. \tag{9}$$

These are listed for our cluster sample in columns 6 and 7 of Table 1. Such values are relevant if one wants to calculate the total mass (M_{tot}) of the pristine cloud that has given birth to both generations, taking into consideration the possible loss of stars through tidal interaction. In the case of the original first stellar generation, this has to be equal to the present mass M_{1G} plus all the stars lost through tidal interactions: $(1 - \alpha_{1G})\epsilon_{1G}M_{tot}$. This through Equation (1) leads to

$$M_{tot} = \frac{M_{1G}}{\epsilon_{1G}\alpha_{1G}}. \tag{10}$$

Similarly, one can consider the mass available for a second stellar generation (Equation (6)) and its likely efficiency of star formation (ϵ_{2G}) and evolution (α_{2G}) parameters, which lead to

$$M_{tot} = \frac{M_{2G}}{(1 - 0.85\epsilon_{1G})\alpha_{2G}\,\epsilon_{2G}} = \frac{M_{2G}}{(1 - 0.85\epsilon_{1G})\alpha_{1G}}\gamma = \frac{M_{2G}X}{\epsilon_{1G}\alpha_{1G}}. \tag{11}$$

Equations (10) and (11) allow for the use of the present mass M_{1G} or M_{2G} to derive the mass M_{tot} of their primordial clouds. Inferring M_{tot} in the case of a GC with multiple subpopulations becomes more complicated as one requires diagrams linking M_{j-1}/M_j with the corresponding increment on ΔY (similar to Figure 1) for each of the subpopulations. We leave a full discussion of such an issue to a forthcoming contribution.

Given the degeneracy in Equation (7) and the lack of other observable(s), the furthest we can reach in our treatment is to

[7] Indeed, we expect that the ongoing photometric survey of multiple stellar populations in GGCs based on the use of ultraviolet photometric filters (which represent a formidable tool for tracing the distinct subpopulations; see Piotto et al. 2015 for a detailed discussion on this issue) can provide more robust empirical estimates on both ΔY and the 1G/2G population ratio.

Table 1
Observed and Derived Parameters for a Sample of GGCs

NGC	ΔY	N_1/N_2 $X \sim M_{1G}/M_{2G}$	M_{GC} $10^6 M_\odot$	ϵ_{1G}	M_{1G} $(10^5 M_\odot)$	M_{2G} $(10^5 M_\odot)$	γ	M_{tot} $(10^6 M_\odot)$
(1)	(2)	(3)	(4)	(5)	(6)	(7)	(8)	(9)
104	0.03	0.43	1.26	0.35	3.78	8.81	0.86	1.26
288	0.013	1.22	0.08	0.18	0.44	0.36	5.64	0.24
2808	0.14	1	1.58	0.78	7.93	7.92	0.43	2.35
5139	0.14	3	3.98	0.78	29.86	9.95	1.28	3.83
6121	0.04	0.56	0.06	0.43	0.23	0.40	0.84	0.06
6397	0.01	0.43	0.25	0.15	0.75	1.76	2.57	0.52
6441	0.07	1	1.58	0.59	7.93	7.92	0.85	1.59
6752	0.035	1.22	0.16	0.39	0.87	0.71	2.09	0.22
7089	0.07	4.88	1.0	0.59	8.3	1.70	4.18	1.42

infer a lower limit to M_{tot}. For clusters to the left of the solid line in Figure 2, we assume the upper-limit value for the product $\epsilon_{2G}\ \alpha_{2G} = 1$, which leads through Equations (10) and (11) to a lower limit on M_{tot}. In this case, α_{1G} is equal to γ for all $\gamma \leqslant 1$.

On the other hand, if instead one assumes the other extreme case, that during the evolution no stars are lost from the first stellar generation ($\alpha_{1G} = 1$), then the product $\epsilon_{2G}\alpha_{2G}$, implicit in Equation (11), has to present values smaller than α_{1G} to lead to values of $\gamma = \alpha_{1G}/(\epsilon_{2G}\alpha_{2G}) \geqslant 1$ in Equation (7). The result is then to displace the mass ratio M_{1G}/M_{2G} from the solid line in Figure 2 toward the right until the present values of X are reached. The derived values of γ for all clusters are given in column 8 of Table 1, and the predicted values of the lower mass limit for M_{tot} (through Equations (9)–(11)) are given in the last column.

4. RESULTS AND DISCUSSION

There are several issues regarding the observational data. Some of the GCs, regardless of their total mass, present a mass M_{2G} larger than M_{1G}, but the opposite, an M_{1G} larger than M_{2G}, is also possible. Both trends also happen for clusters with a similar value of ΔY. Note also clusters with a similar mass ratio but a different ΔY value. In our approach, some of the GCs can only be explained if γ acquires large values, implying that the product $\epsilon_{2G}\alpha_{2G}$ should lead to a low value, reaching ~0.1 to encompass our selected clusters. On the other hand, some GCs are required to expel through tidal effects a large fraction of their stars from 1G, so γ reaches values of ~0.5 to encompass our clusters.

Taking the observational data at face value, note that only four clusters are to the left of the solid line in Figure 2, and they all present a mass ratio $M_{1G}/M_{2G} \leqslant 1$. In principle there is no physical restriction for this upper limit ($M_{1G}/M_{2G} \leqslant 1$), and thus perhaps more data points are needed. Three of the four clusters to the left of the solid line (NGC 104, NGC 6121, and NGC 6441) are in fact almost at the solid line (with values of γ ~0.85) and have their predicted lower-limit mass M_{tot} almost identical to the present total mass (M_{GC}). This happens despite the fact that they present a different total mass (M_{GC}), a different mass ratio (X), and a different ϵ_{1G}. This indeed supports the interpretation that there has hardly been any evolution or loss of stars through tidal interactions from either generation and that the efficiency of star formation of the second stellar generation was rather large (see Equation (7)). The case of NGC 2808 is different as it implies a value of γ ~0.43, and thus despite its value of $X = 1$, it must have suffered a major loss of stars from its first generation, which agrees with having a predicted lower-limit total mass (M_{tot}) larger than the present mass of the cluster.

The other five clusters in the sample are to the right of the solid line and cover a large range of X values. One can compare NGC 2808 with NGC 5139. Both have the same value of ΔY and thus the same ϵ_{1G}. However, the former is to the left of the solid line and the latter to the right, with a mass ratio $X = 3$. The latter is the only cluster in the whole sample for which the predicted M_{tot} is slightly smaller (by about 4%) than the total present mass of the cluster. However, having M_{1G} larger than M_{2G} implies it is most likely that no stars were lost from either generation, and its low value of $\alpha_{2G}\ \epsilon_{2G}$ comes from a low value of ϵ_{2G} (~0.77), which leads to $\gamma = 1.29$. A similar case is that of NGC 6441 and NGC 7089, each having the same value of ΔY. As mentioned above, NGC 6441 has hardly evolved at all, and thus its predicted M_{tot} is almost identical to the observed mass M_{GC}. The location of NGC 7089 with an M_{1G} much larger than M_{2G} implies a very low efficiency in the second stellar generation, perhaps due to the dispersal of a large amount of contaminated gas (several times $10^5\ M_\odot$), which was unable to enhance the mass of the 2G.

To appreciate the range of possible evolutions, one should consider also NGC 6441 and NGC 7089, both presenting a $\Delta Y = 0.070$. They both have a similar predicted lower-limit mass M_{tot}, and both gave origin to very similar, massive first generations. However, NGC 6441 led to a massive second stellar generation (and presents a mass ratio $X \sim 1$), while in NGC 7089 the second generation is almost five times smaller than the first.

Low-mass clusters such as NGC 6397 and NGC 288 present the lowest values of ΔY and thus the lowest $\epsilon_{1G} = 0.146$ (see Table 1). If one deducts from the predicted initial total mass the mass of the observed first generation, one would have, in principle, an estimate of the mass left for a second stellar generation. NGC 288 with a leftover mass of $\sim 1.99 \times 10^5\ M_\odot$ only used less than 20% of it for its 2G, reaching an X value of 1.22, while NGC 6397 with an available mass $\sim 4.4 \times 10^5\ M_\odot$ transformed almost 40% of it for its 2G and has an X value equal to 0.43.

In summary, the location of GGCs in the ΔY versus M_{1G}/M_{2G} diagram points in the cases close to the solid line (see Figure 2) to a lack of evolution. Their predicted lower mass limit (M_{tot}) is almost identical to the present mass of the GCs (M_{GC}). We have also pointed out clusters to the left of the solid line, which can only be justified if there is a major loss of stars from the first stellar generation. And finally, all clusters to the

right of the solid line require, most likely, a low star-formation efficiency for the second stellar generation (ϵ_{2G}) to justify the range of values of their mass ratios. All these possibilities may have different origins. GCs have clearly been affected throughout their evolution in different manners, perhaps due to some initial structural parameters, such as the size of the star-formation event or the location of their orbit around the Galaxy center, that may have allowed for very different histories of tidal interactions.

Note that so far we have only considered stars with a mass $M_* \leqslant 1\,M_\odot$, the stars we see today. However, to account for the full IMF required to cause the contamination of the 2G and also its full IMF, one would have to add an extra 62% to the derived values of $M_{\rm tot}$ (see Table 1) to obtain the 100% original mass of the clouds that gave birth to the original massive starbursts that after their extended evolution appear today as GGCs. The range is then defined in our sample by NGC 6121 and NGC 5139, which indicate the full mass of the primordial clouds ranging from $1.66\times10^5\,M_\odot$ to $1.01\times10^7\,M_\odot$.

5. CONCLUDING REMARKS

We depart from a massive cloud that after gravitational collapse gives origin to a first stellar generation with a full IMF. Some of these stars shed their H-burning products and contaminate the gas left over from star formation. We have used for this the products from massive interacting binaries, assuming that about 15% of the total mass of the IMF becomes then available to contaminate the remaining cloud. Other contaminants may also be used, changing in our equations the amount of mass (M_c) and the appropriate Y_c value expected from these other alternatives. The remaining cloud is assumed to be strongly centrally concentrated with a gas distribution that promotes the blowout of SN blast waves from first-generation massive stars and thus the exit of the ejected matter from the cluster volume (as in Tenorio-Tagle et al. 2015).

In our models, the efficiency of star formation of the first stellar generation (ϵ_{1G}) is the variable that fully defines and links the stellar generations in a GC, first because it defines the number of stars in the 1G, and second because it fixes concurrently the amount of gas left over while defining the mass available for its contamination. Furthermore, we have shown that ϵ_{1G} is fully defined by the observations because it only depends on ΔY (see Equation (5)).

We have also shown that the location of GCs in a ΔY versus M_{1G}/M_{2G} diagram provides information about their formation and evolution as a variable γ in Equations (7) and (8) fully defined by the observations. Clusters to the left of the solid line in Figure 2 can only be there if the cluster loses, through tidal interactions, a good fraction of its 1G stars. On the other hand, clusters to the right of the solid line may only lie there as a result of a poor efficiency of stellar formation in their second stellar generation, a fact that is reinforced by the empirical evidence of having the second generation strongly centrally concentrated and thus clearly unable to have lost its stars. Clusters at or near the solid line on Figure 2 do not lose stars from either generation, as confirmed by the fact that their present mass is equal to the here-predicted lower-limit total mass of their primordial cloud ($M_{\rm tot}$). This accounts only for the low-mass stars (38% of the full IMF), and thus to obtain a true $M_{\rm tot}$ one should add an extra 62% to have the full mass of the primordial clouds that gave origin to GGCs.

On the basis of the present analysis, we suggest the use of the ΔY versus M_{1G}/M_{2G} diagram as a powerful tool for tracing the formation and evolution properties of Galactic GCs.

This study was supported by CONACYT–México, grants 167169 and 131913, and by the Spanish Ministry of Science and Innovation for the ESTALLIDOS collaboration (grants AYA2010-21887-C04-04 estallidos4 and AYA2013-47742-C4-2-P estallidos5). GTT and SC acknowledge the Cátedra Severo Ochoa at the Instituto de Astrofísica de Canarias, and GTT also thanks the Jess Serra Foundation and the CONACYT grant 232876 for a sabbatical leave. SC acknowledges financial support from PRIN-INAF 2014 (PI: S. Cassisi), the friendly hospitality at the IAC, and very helpful discussions with M. Salaris. The authors appreciate the science and discussions among the participants of the ESTALLIDOS Star Formation Feedback Workshop (IAC, 2014 November), which triggered a good number of ideas.

REFERENCES

Bastian, N., Cabrera-Ziri, I., & Salaris, M. 2015, MNRAS, 449, 3333
Bastian, N., Lamers, H. J. G. L. M., de Mink, S. E., et al. 2013, MNRAS, 436, 2398
Bastian, N., & Lardo, C. 2015, MNRAS, 453, 357
Beck, S. 2015, IJMPD, 24, 1530002
Bedin, L. R., Piotto, G., Anderson, J., et al. 2004, ApJ, 605, L125
Bellini, A., Bedin, L. R., Piotto, G., et al. 2010, AJ, 140, 631
Bellini, A., Piotto, G., Bedin, L. R., et al. 2009, A&A, 493, 959
Bellini, A., Piotto, G., Milone, A. P., et al. 2013, ApJ, 765, 32
Calura, F., Few, C. G., Romano, D., & D'Ercole, A. 2015, ApJL, 814, L14
Carretta, E., Bragaglia, A., Gratton, R. G., et al. 2009, A&A, 505, 117
Cassisi, S., Mucciarelli, A., Pietrinferni, A., Salaris, M., & Ferguson, J. 2013a, A&A, 554, A19
Cassisi, S., Salaris, M., & Pietrinferni, A. 2013b, MmSAI, 84, 91
Dalessandro, E., Massari, D., Bellazzini, M., et al. 2014, ApJL, 791, L4
D'Antona, F., Caloi, V., Montalbán, J., Ventura, P., & Gratton, R. 2002, A&A, 395, 69
de Mink, S. E., Pols, O. R., Langer, N., & Izzard, R. G. 2009, A&A, 507, L1
D'Ercole, A., D'Antona, F., & Vesperini, E. 2011, MNRAS, 415, 1304
D'Ercole, A., Vesperini, E., D'Antona, F., McMillan, S. L. W., & Recchi, S. 2008, MNRAS, 391, 825
Dotter, A., Ferguson, J. W., Conroy, C., et al. 2015, MNRAS, 446, 1641
Gratton, R. G., Carretta, E., & Bragaglia, A. 2012, A&ARv, 20, 50
Izzard, R. G., de Mink, S. E., Pols, O. R., et al. 2013, MmSAI, 84, 171
King, I. R., Bedin, L. R., Cassisi, S., et al. 2012, AJ, 144, 5
Krause, M., Charbonnel, C., Decressin, T., et al. 2012, A&A, 546, L5
Kroupa, P. 2001, MNRAS, 322, 231
Lardo, C., Bellazzini, M., Pancino, E., et al. 2011, A&A, 525, A114
Larsen, S. S., de Mink, S. E., Eldridge, J. J., et al. 2011, A&A, 532, A147
Marino, A. F., Milone, A. P., Piotto, G., et al. 2012, ApJ, 746, 14
Marino, A. F., Milone, A. P., Przybilla, N., et al. 2014, MNRAS, 437, 1609
Marino, A. F., Sneden, C., Kraft, R. P., et al. 2011, A&A, 532, A8
Marino, A. F., Villanova, S., Piotto, G., et al. 2008, A&A, 490, 625
Milone, A. P., Marino, A. F., Dotter, A., et al. 2014, ApJ, 785, 21
Milone, A. P., Marino, A. F., Piotto, G., et al. 2012a, ApJ, 745, 27
Milone, A. P., Marino, A. F., Piotto, G., et al. 2013, ApJ, 767, 120
Milone, A. P., Marino, A. F., Piotto, G., et al. 2015, MNRAS, 447, 927
Milone, A. P., Piotto, G., Bedin, L. R., et al. 2012b, ApJ, 744, 58
Milone, A. P., Piotto, G., Bedin, L. R., et al. 2012c, A&A, 540, A16
Milone, A. P., Piotto, G., King, I. R., et al. 2010, ApJ, 709, 1183
Norris, J. E. 2004, ApJL, 612, L25
Piotto, G., Bedin, L. R., Anderson, J., et al. 2007, ApJL, 661, L53
Piotto, G., Milone, A. P., Anderson, J., et al. 2012, ApJ, 760, 39
Piotto, G., Milone, A. P., Bedin, L. R., et al. 2015, AJ, 149, 91
Piotto, G., Milone, A. P., Marino, A. F., et al. 2013, ApJ, 775, 15
Piotto, G., Villanova, S., Bedin, L. R., et al. 2005, ApJ, 621, 777
Renzini, A., D'Antona, F., Cassisi, S., et al. 2015, MNRAS, 454, 4197
Sbordone, L., Salaris, M., Weiss, A., & Cassisi, S. 2011, A&A, 534, A9
Schneider, F. R. N., Izzard, R. G., de Mink, S. E., et al. 2014, ApJ, 780, 117
Tenorio-Tagle, G., Muñoz-Tuñón, C., Silich, S., & Cassisi, S. 2015, ApJL, 814, L8
Turner, J. L., Beck, S. C., Benford, D. J., et al. 2015, Natur, 519, 331